

Performance Evaluation of Computer Simulated Extracted Features of Induction Motor with Intermediate State of Degradation Present in Any Two-Phases

Amit J. Modak, H. P. Inamdar

Abstract— The state of degradation of stator groundwall insulation in induction motor results in the state of unbalance in three-phase stator current at fundamental frequency. In this investigation, the computer simulation model to determine this state of unbalance is developed. On the basis of park's transformation model the unbalanced stator current data in three-phase machine variable ('abc') form is first transformed into equivalent two-phase ('dq') model form. The park's current vector components are then presented in a graphical dq-data pattern form and certain mathematical parameters are deduced. The computer simulation model is designed to extract simulated electrical variables and mathematical parameters of induction motor under test. The practical assumption of stator winding of induction motor being star (Y) connected with isolated neutral is considered. The extracted features of induction motor for particular case of variation in the state of degradation of stator groundwall insulation occurring in respective phases is presented. The performance evaluation of extracted features for the variation in the state of degradation of insulation in one particular phase from healthy to worst-case state along with an arbitrary intermediate state of degradation of insulation present in other two-phases is presented. On the basis of performance evaluation, it is possible to determine the appropriate selection of specific input parameter for optimal design of suitable artificial neural network classifier to distinguish the probable states of degradation of insulation.

Index Terms— computer simulation, induction motor, insulation degradation, park's current transformation, stator groundwall insulation

1 INTRODUCTION

THE stator insulation system¹ of a motor or generator consists of strand and turn insulation, as well as groundwall insulation. The groundwall is the primary insulation, separating the high voltage copper conductors from the grounded steel core. Modern machines use mica flake or mica paper tapes bonded with epoxy or polyester resin as the groundwall insulation. In addition to these components, the insulation system of a bar or coil also includes a semi conductive coating over the slot-section groundwall, with a special coating at the ends of the slots to grade the electric stress in this region. These insulation failures are usually the result of gradual deterioration of the insulation due to aging. The aging results from electrical, mechanical and thermal stresses. The diagnostic tests and measurements to assess the condition of stator winding insulation in a particular machine are mainly classified in two broad categories destructive tests and nondestructive tests. Both the type of test measures are as such relatively insensitive life indicators of stator winding insulation, which still have significant remaining life [1].

More or less the credibility in estimating the insulation condition under nondestructive tests must be correlated with the results of destructive tests [2]. In the previous investigations it is ascertained that there is no correlation between the results of any nondestructive type of (dc / ac) assessment parameters with destructive type of (dc / ac / impulse) breakdown levels [1]. There is a need to establish an economical nondestructive test method for an assessment of state of degradation of stator groundwall insulation caused due to various factors in an integrated way. This is particularly true in case of large numbers of low / medium capacity induction motors operating in variable speed drive environment in any continuous process industry.

2 FORMULATION OF WORK WITH SUGGESTED APPROACH

In view of the above perspective, the present research work presents a novice nondestructive method to assess the state of degradation of stator winding insulation. The method is based on the concept that the degradation occurring in any one of the phases of stator winding insulation, effectively results in the state of unbalance in the three-phase stator current at fundamental supply frequency. The state of degradation of insulation, occurring on account of several reasons, in an integrated way can be readily represented in terms of magnitude and degree of unbalance in the stator current at fundamental supply frequency. The emphasis is towards the

-
- Amit J. Modak is registered as a Ph. D. Research Student in Electrical Engineering at Walchand College of Engineering, Sangli, India with Shivaji University, Kolhapur, INDIA. (E-mail: amitjmodak2000@yahoo.co.in).
 - H. P. Inamdar is working as a Research Professor in Electrical Engineering at Rajarambapu Institute of Technology, Rajaramnagar, District-Sangli, Maharashtra, INDIA and associated as research Ph. D. guide with Shivaji University, Kolhapur, INDIA. (E-mail: inamdar_hp@yahoo.co.in).

application of such unbalanced stator current numerical data to a suitable artificial intelligence (AI) based tool to determine the state of degradation of stator insulation. On experimental basis it is not feasible to collect the large set of unbalanced stator current data, which would model the entire range of state of degradation of insulation for the specific motor used in particular industry. However, in neural network based AI-technique, a large set of data pattern availability is required for the development of diagnostic model to detect the state of degradation of stator groundwall insulation. This is essential from the point of view of optimal design and efficient performance of the neural network classifier. Hence, there is need to generate large number of unbalanced stator current numerical data on the basis of computer simulation model to represent the various states of degradation of stator groundwall insulation occurring in respective phases. The formulation and execution of computer simulation model to generate unbalanced stator current data pattern was done in the previous work [3]. In the previous work, the modeling was based on the assumption that the stator winding was star-connected with grounded neutral. As against this, in the present investigation, based on the similar approach, the formulation of computer simulation model is derived based on the practical condition of isolated neutral. The modeling is done for three-phase, cage-rotor, 10-HP, star (Y)-connected a. c. induction motor used in a continuous process industry.

In general, the motor operates under the presence of many internal and external recipient faults. In the spectrum analysis based fault diagnosis techniques [4], [5], it is concluded that these faults are observable at some definite frequencies, which are different than the supply frequency. These stator winding faults are present due to several causes like inter-turn short circuit insulation failure [6], air gap eccentricity [7] etc; but not on account of degradation of stator groundwall insulation. The state of degradation of stator groundwall insulation of the respective phase results into the reduction of resistance to the thermal conductivity. This results into an increase in the rate of heat transfer from the surface of the stator winding conductors to the remaining part of the structure. This excessive heat loss to the surroundings is interpreted as the motor is subjected to excessive copper losses bearing the loss in efficiency at the supply frequency. Hence, motor draws more current as compared to what it would have drawn had the insulation not degraded. In view of the above reasons, the increase in current in respective phases leads to an unbalance in stator current at fundamental supply frequency.

The increase in current is accompanied as reduction in the steady-state equivalent resistance of motor referred to stator. The state of degradation of insulation of the respective phase, also results in the increase in the leakage current. This is on account of decrease in the magnetizing reactance (i.e., " X_m ") component. The combined effect of the above two factors is interpreted as the reduction in the real part of the equivalent impedance of the motor referred to stator under the absence of mechanical load condition. The imaginary part of the equivalent impedance of the motor referred to stator under the absence of mechanical load condition will not change much since the inductance does not contribute to the dissipation of

any energy on account of loss of heat to the surroundings. In the present work, as shown in the Fig. 1 below, the reduction in the real part of an equivalent impedance of motor referred to stator under the absence of mechanical load condition (i.e., "Real ($Z_{seq1_im_nl}$)") is simulated by the presence of suitable values of variable shunt resistance (i.e., " R_{sh} ") connected across it in the lumped form.

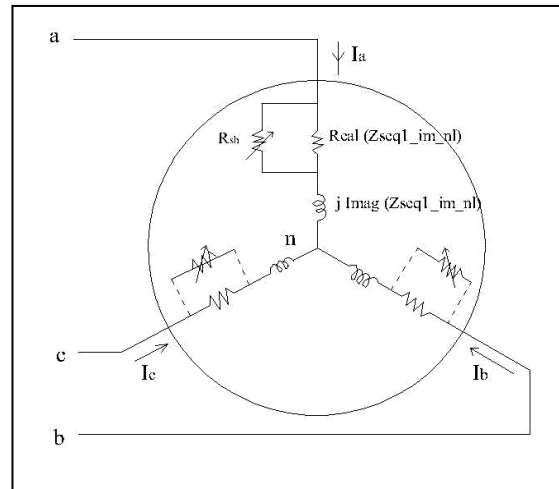


Fig. 1. Simulation of State of Degradation of Stator Groundwall Insulation of Respective Phase with Isolated Neutral

The computer simulation program is designed to generate unbalanced three-phase stator current data pattern on the basis of the resultant steady-state equivalent motor impedance per-phase. The resultant stator current data pattern is simulating the specific state of degradation of stator groundwall insulation of the respective phases of the motor under test. The computer simulation program incorporates the feature of extended park's transformation model to transform the three-phase unbalanced stator current data patterns in the three-phase ('abc') machine variable form into two-phase ('dq') park's current vector component form. The graphical representations of resultant park's current dq-data pattern forms are illustrated. The computer simulation model is designed further to execute the extraction of various electrical variables and mathematical parameters, which specifically distinguish the state of degradation of stator groundwall insulation of respective phases. The detailed analysis and the summary of the series of extracted variables and mathematical parameters are presented for the particular case of the state of degradation of stator groundwall insulation.

3 COMPUTER SIMULATION FOR EVALUATION OF STATE OF DEGRADATION OF STATOR GROUNDWALL INSULATION

The simulation model is designed on the basis of certain assumptions and reference conditions in context to the representation of balanced line voltages and the resulting unbalanced phase voltages and stator currents, over a phase plane.

3.1 Nomenclature

The nomenclature of various variables involved in the simulation model is detailed as under. The representation of the electrical variables over a phase plane is as shown in Fig. 2. The bold face symbolic representation of respective variables represents their corresponding RMS values.

V_{ab}, V_{bc}, V_{ca} The absolute values of three-phase, balanced, line-to-line supply voltages across the respective phases (viz., 'a, b, and c' of star-(Y) connected stator winding with isolated neutral, respectively.), in 'Volts.'

V_a, V_b, V_c The absolute values of phase-voltages across the phases (viz., 'a, b, and c' of star-(Y) connected stator winding with respect to isolated neutral, respectively.), in 'Volts.'

$\alpha_a, \alpha_b, \alpha_c$ The phase angles of phase-voltages across the phases (viz., 'a, b, and c' respectively.), expressed in electrical degrees ('°').

I_a, I_b, I_c The absolute values of stator current per-phase of the phases (viz., 'a, b, and c' respectively.), in 'Amps.'

$\beta_a, \beta_b, \beta_c$ The phase angles of phase-currents of the phases (viz., 'a, b, and c' respectively.), expressed in electrical degrees ('°').

Z_a, Z_b, Z_c The absolute values of steady-state equivalent motor impedances per-phase referred to stator for the operation of motor under the absence of mechanical load condition corresponding to some finite values of shunt resistances ('Rsh') between maximum (viz., close to infinity-∞) and minimum value (viz., close to zero-0), in ohms ('Ω').

Z_0 The absolute value of steady-state equivalent motor impedance per-phase referred to stator for the operation of motor under the absence of mechanical load condition, for the value of shunt resistance ('Rsh') equal to infinity (∞), in ohms ('Ω').

I_d, I_q, I_0 The absolute values of direct-axis, quadrature-axis, and zero-sequence current per-phase of the equivalent '2-phase' machine ('dqo') model, respectively, in ('Amps.').

β_d, β_q The phase angles of 'direct-axis' and 'quadrature-axis' current per-phase of the equivalent '2-phase' machine ('dqo') model, respectively, in electrical degrees ('°').

I_{dq} The absolute value of resultant of the 'direct-axis' and 'quadrature-axis' current component per-phase of the equivalent '2-phase' machine ('dqo') model, in ('Amps.').

β_{dq} The phase angle of resultant of 'direct-axis' and 'quadrature-axis' current component per-phase of the equivalent '2-phase' machine ('dqo') model, expressed in electrical degrees ('°').

L_{MA}, L_{MB}, LR The length of major axis ('LMA'), length of minor axis ('LMB'), and latus rectum ('LR') of extended park's current data pattern, in ('Amps.').

ϵ Eccentricity ('ε') of extended park's current data pattern.

θ_0° Orientation angle of extended park's current data pattern (locus), measured with respect to reference with anti-clockwise sense as positive, expressed in electrical degrees ('°').

θ_m° Angle of major axis of extended park's current data pattern, measured with respect to reference axis with anti-clockwise sense as positive, in electrical degrees ('°').

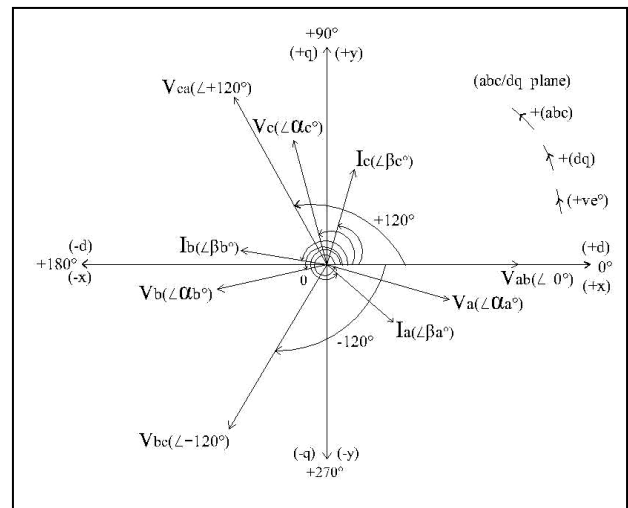


Fig. 2. Phase Plane Representation of Electrical Variables

3.2 Determination of Steady- State Unbalanced Stator Currents Per-Phase

The computer simulation of steady-state equivalent circuit of induction motor with rotor at stator frequency is done on 'MATLAB.' The measured machine parameters are used to assess the performance of cage-rotor induction motor in the machine variable form under minimum mechanical load condition. The minimum mechanical load condition is realized under the absence of mechanical load, by decoupling the mechanical load from the shaft of motor. Simulation analysis was conducted on three-phase, 10HP (7.5-kW), star (Y)-connected, six-pole, induction motor. The steps involved in the development of simulation model for the evaluation of state of degradation of insulation are as under-

- Determination of machine parameters for induction motor under test.
- The computation of steady state performance of induction motor in machine variable form under minimum mechanical load condition.
- Evaluation of maximum and minimum values of shunt resistances across the real part of equivalent steady-

state motor impedance per-phase referred to stator side at stator frequency under minimum mechanical load condition.

- The computation of the numerical values of number of shunt resistances between maximum and minimum values, which are simulating different state of degradation of stator groundwall insulation.
- The numbers of steady-state equivalent motor impedances per-phase referred to stator side (i.e., "Zseq1_im_nl_xd") under the absence of mechanical load condition are computed for the range of values of shunt resistances (i.e., "R_{sh}") within maximum and minimum values. The simulation results for the same computations are presented in Table-1.

TABLE 1

SIMULATION RESULTS OF STEADY-STATE MOTOR IMPEDANCES PER-PHASE

R _{sh} (Ω)	Percentage of Reduction in Real Part of (Zseq1_im_nl) (%)	Absolute Value of Zseq1_im_nl_xd (Ω)
∞	0	36.7698
608.1699	5	35.3853
288.0805	10	34.0198
96.0268	25	30.0627
48.0134	40	26.3873
32.0089	50	24.1575
21.3393	60	22.167
10.6696	75	19.7858
3.5565	90	18.3763
1.6847	95	18.166

As shown in the 'Table-1,' the absolute value of steady-state motor impedance per-phase corresponding to an infinite (∞) value of shunt resistance (R_{sh}), represents the healthy state of stator groundwall insulation of the respective phase. Similarly, the absolute value corresponding to some finite minimum value of shunt resistance i.e., 1.6847 (Ω) represents a finite worst-case state of degradation of stator groundwall insulation of the respective phase. The absolute value corresponding to the value of shunt resistance anything in between finite maximum and minimum value represents an arbitrary intermediate state of degradation of the respective phase. The numbers of combinations of these numerical values of steady state equivalent motor impedances per-phase referred to stator are determined to model the numbers of various states of degradation. The overall percentage of degradation (i.e., "per_xd (%)") is represented in numerical form by the concept of root mean square value of absolute deviation of impedances (i.e., "Z_{xd} (Ω)") in three phases. The same is now proposed with the following analytical definition.

$$Z_{xd} = \left(\sqrt{\frac{(Z_0 - Z_a)^2 + (Z_0 - Z_b)^2 + (Z_0 - Z_c)^2}{3}} \right) \times 100$$

$$per_xd (\%) = (Z_{xd} / Z_0) \times 100$$

(1)

The simple subroutine program is designed to determine numbers of such possible combinations for respective phases. These numbers of combinations of steady-state motor impedances per-phase are used further to compute the stator currents per-phase. The resulting unbalanced stator currents per-phase are computed under the condition of balanced supply voltage of star-(Y) connected stator winding with isolated neutral viz., (2) and (3).

$$V_{ab} + V_{bc} + V_{ca} = 0$$

(2)

$$I_a + I_b + I_c = 0$$

(3)

The equations for the corresponding stator currents for the respective phases based on condition (2) and (3) are derived as under-

$$I_a = \left((Z_b + Z_c)V_{ab} + Z_bV_{bc} \right) / (Z_aZ_b + Z_bZ_c + Z_cZ_a)$$

(4)

$$I_b = \left(-Z_cV_{ab} + Z_aV_{bc} \right) / (Z_aZ_b + Z_bZ_c + Z_cZ_a)$$

(5)

$$I_c = - \left(Z_bV_{ab} + (Z_a + Z_b)V_{bc} \right) / (Z_aZ_b + Z_bZ_c + Z_cZ_a)$$

(6)

The computer simulation program is designed to generate around 'm=8000' number of unique combinations of unbalanced three-phase stator current data pattern. Each one of these data pattern is simulating the specific state of degradation of stator groundwall insulation of the respective phases of the motor under test. The simulation results of motor variables like- overall percentage of degradation of insulation (i.e., "per_xd (%)") in the form of matrix (i.e., "[per_xd]_{mxi}"), absolute value of steady-state motor-impedances per-phase for respective phases in the form of matrix (i.e., "[Z_a Z_b Z_c]_{mx3}") in Ω, absolute values and phase-shift angles of stator current per-phase for respective phases in the form of matrix (i.e., "[I_a I_b I_c β_a β_b β_c]_{mx6}") in amperes and electrical degrees, respectively, are detailed in 'Table-2.' The 'Table-2,' represents the simulation data for few numbers (No.) of unique combinations of unbalanced three-phase stator currents for the particular case of equal intermediate state of degradation of insulation present in any two-phases with variation in the state of degradation of insulation in the remaining phase.

3.3 Extended Park's Current Transformation Model for Computation of Direct-axis and Quadrature-axis Current Components

The park's current vector pattern learning approach has been successfully applied in the fault diagnosis of ac induction motor drive [7], [8]. In this investigation, the same approach is

applied for the presentation of various states of degradation of induction motor. insulation, occurring in respective phases of stator winding of

TABLE 2

SIMULATION RESULTS OF ELECTRICAL VARIABLES IN THREE-PHASE MACHINE MODEL (ABC) FORM FOR EQUAL INTERMEDIATE STATE OF DEGRADATION OF INSULATION PRESENT IN PHASE-B AND PHASE-C WITH VARIABLE STATE OF DEGRADATION IN PHASE-A

No.	per_xd (%)	Z _a (Ω)	Z _b (Ω)	Z _c (Ω)	I _a (A)	β _a (°)	I _b (A)	β _b (°)	I _c (A)	β _c (°)
1	0.00	36.7698	36.7698	36.7698	6.5162	300.519	6.5162	180.519	6.5162	60.5195
211	28.0063	36.7698	24.1575	24.1575	7.4334	295.847	10.1698	170.755	8.4712	36.6448
2211	29.9209	30.0627	24.1575	24.1575	8.5637	289.702	10.1301	166.760	9.0337	39.4688
3411	32.4055	26.3873	24.1575	24.1575	9.3517	285.068	10.0326	163.770	9.52	40.8449
4211	34.3005	24.1575	24.1575	24.1575	9.9182	281.491	9.9182	161.491	9.9182	41.4911
5011	36.1951	22.167	24.1575	24.1575	10.5088	277.471	9.7498	158.970	10.3786	41.8243
6211	38.6720	19.7858	24.1575	24.1575	11.4059	270.525	9.363	154.766	11.1776	41.5503
7811	40.4678	18.166	24.1575	24.1575	12.4828	259.482	8.5178	148.698	12.3658	39.3924

As shown in Fig. 3, the park's transformation model, transforms the presentation of unbalanced stator current data pattern in three-phase ('abc') machine variable form into two-phase ('dq') machine variable form over a phase-plane.

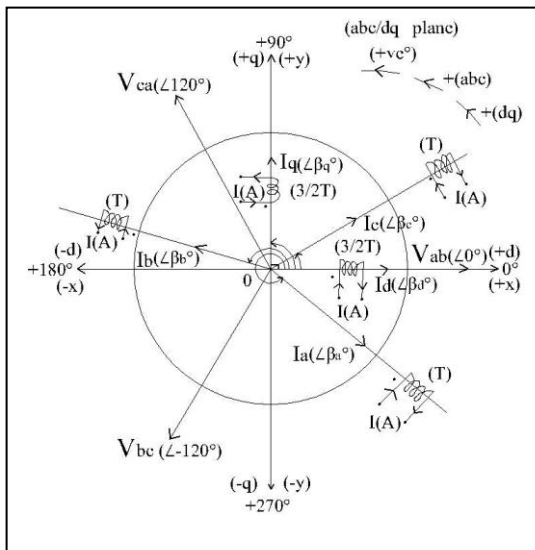


Fig. 3. Extended Park's Current Transformation Model

For uniqueness of the transformation from one set of axes to another set of axes, including the unbalances in the 'abc' variables requires three variables such as 'dq0'. The relationship between 'dq0' and 'abc' current variables is derived as follows-

$$\begin{bmatrix} I_d \\ I_q \\ I_0 \end{bmatrix} = \frac{2}{3} \begin{bmatrix} \cos(\beta_a^\circ) & \cos(\beta_b^\circ) & \cos(\beta_c^\circ) \\ \cos(\beta_a^\circ - 90^\circ) & \cos(\beta_b^\circ - 90^\circ) & \cos(\beta_c^\circ - 90^\circ) \\ 1/2 & 1/2 & 1/2 \end{bmatrix} \begin{bmatrix} I_a \\ I_b \\ I_c \end{bmatrix} \quad (7)$$

The zero-sequence current 'I₀' (A) represents the imbalance in the 'phase-a, phase-b, and phase-c' currents. Under the practical condition of star (Y) connected stator winding with isolated neutral, the zero-sequence current component is always equal to zero and does not produce the resultant magnetic field. The relationship between 'dq0' and 'abc' currents is modified as follows-

$$\begin{bmatrix} I_d \\ I_q \end{bmatrix} = \frac{2}{3} \begin{bmatrix} \cos(\beta_a^\circ) & \cos(\beta_b^\circ) & \cos(\beta_c^\circ) \\ \cos(\beta_a^\circ - 90^\circ) & \cos(\beta_b^\circ - 90^\circ) & \cos(\beta_c^\circ - 90^\circ) \end{bmatrix} \begin{bmatrix} I_a \\ I_b \\ I_c \end{bmatrix} \quad (8)$$

The extended park's current transformation model detailed in (8) is included in computer simulation program to compute park's current data pattern for all possible combinations of unbalanced three-phase stator currents. The simulation results of extended park's current data pattern for particular case of equal intermediate state of degradation of insulation present in any two-phases with variable state of degradation occurring in the remaining phase of induction motor under test are listed in 'Table-3.' The graphical representations of extended park's current data pattern are in an elliptic form. The computer program is designed further to extract certain mathematical parameters like length of major axis (L_{MA}), length of minor axis (L_{MB}), eccentricity (ε), latus rectum (LR), angle of major axis (θ_m°), and orientation angle (θ₀°) of extended park's current data pattern (locus). The extracted parameters are listed in 'Table-4.' The extended park's current data patterns, presented in terms of simplified electrical variables in two-phase machine model form (refer 'Table-3') and extracted mathematical parameters (refer 'Table-4') of selected number of combinations of unbalanced three-phase stator currents, are used to analyze and distinguish various states of degradation of insulation of respective phases for the induction motor under test. The performance analysis is detailed with the support of graphical representations in the following sections.

TABLE 3

SIMULATION RESULTS OF ELECTRICAL VARIABLES IN EQUIVALENT TWO-PHASE MACHINE MODEL (DQ) FORM FOR EQUAL INTERMEDIATE STATE OF DEGRADATION OF INSULATION PRESENT IN PHASE-B AND PHASE-C WITH VARIABLE STATE OF DEGRADATION IN PHASE-A

No.	per_xd (%)	Z _a (Ω)	Z _b (Ω)	Z _c (Ω)	I _d (A)	β _d (°)	I _q (A)	β _q (°)	I _{dq} (A)	β _{dq} (°)
1	0.00	36.7698	36.7698	36.7698	6.5162	360	6.5162	90	9.2153	45
211	28.0063	36.7698	24.1575	24.1575	11.1869	358.38	6.2084	92.9075	12.3589	28.4386
2211	29.9209	30.0627	24.1575	24.1575	10.6433	358.04	7.8562	92.6436	12.7123	36.0746
3411	32.4055	26.3873	24.1575	24.1575	10.2217	358.76	9.0529	91.3911	13.3404	41.4472
4211	34.3005	24.1575	24.1575	24.1575	9.9182	0	9.9182	90	14.0265	45
5011	36.1951	22.167	24.1575	24.1575	9.6303	2.1305	10.8072	88.1016	14.972	48.1883
6211	38.6720	19.7858	24.1575	24.1575	9.3618	7.501	12.078	84.1925	16.899	51.5698
7811	40.4678	18.166	24.1575	24.1575	9.8212	17.883	13.2455	76.8389	20.1513	52.1578

TABLE 4

SIMULATION RESULTS OF EXTRACTED MATHEMATICAL PARAMETERS FOR EQUAL INTERMEDIATE STATE OF DEGRADATION OF INSULATION PRESENT IN PHASE-B AND PHASE-C WITH VARIABLE STATE OF DEGRADATION IN PHASE-A

No.	per_xd (%)	Z _a (Ω)	Z _b (Ω)	Z _c (Ω)	θ ₀ (°)	θ _m (°)	L _{MA} (A)	L _{MB} (A)	ε	LR (A)
1	0.00	36.7698	36.7698	36.7698	90	90	13.0325	13.0325	0	13.0325
211	28.0063	36.7698	24.1575	24.1575	92.9075	-3.6012	22.4046	12.3613	0.834	6.8201
2211	29.9209	30.0627	24.1575	24.1575	92.6436	-7.2222	21.3668	15.6031	0.6832	11.3942
3411	32.4055	26.3873	24.1575	24.1575	91.3911	-10.7394	20.5183	18.0207	0.4782	15.8271
4211	34.3005	24.1575	24.1575	24.1575	90	90	19.8365	19.8365	0	19.8365
5011	36.1951	22.167	24.1575	24.1575	88.1016	73.8695	21.8029	19.0469	0.4867	16.6393
6211	38.6720	19.7858	24.1575	24.1575	84.1925	68.6066	24.9642	17.6314	0.7079	12.4525
7811	40.4678	18.166	24.1575	24.1575	76.8389	59.8034	29.2414	15.2494	0.8533	7.9525

The graphical representations of an extended park's current data pattern, for a particular class of equal variation in the state of degradation of insulation, occurring in all the three respective phases are in the circular form with centre at the origin over a dq-plane. The ideal condition refers to zero-percent ('0 %') state of degradation of stator groundwall insulation, occurring in all the three respective phases. The associated electrical variables and extracted mathematical parameters for this state of reference are presented by the combination 'no.1' in the 'Table-2, Table-3, and Table-4.' The extended park's current data pattern representation over a dq-plane is as illustrated in Fig. 4. The variations are observed with respect to circular extended park's current data pattern corresponding to combination 'no.1' as a state of reference.

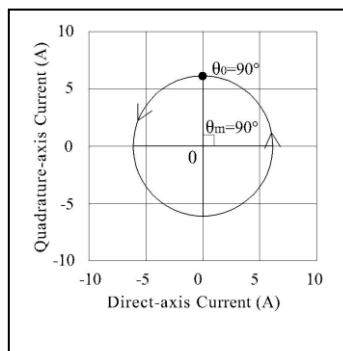


Fig. 4. Circular Extended Park's Current Data Pattern as a Reference to Simulate Zero-Percent of State of Degradation.

4 EQUAL INTERMEDIATE STATE OF DEGRADATION OF INSULATION PRESENT IN ANY TWO-PHASES WITH VARIABLE STATE OF DEGRADATION IN REMAINING PHASE

The graphical representations of extended park's current data pattern for equal intermediate state of degradation of insulation present in any two-phases with variable state of degradation, occurring in the remaining phase are in an elliptic form with centre at origin over a dq-plane. In the present work, the '50%' reduction in the real part of steady-state motor impedance per-phase is considered to represent an arbitrary intermediate state of degradation of stator groundwall insulation of the respective phase. The corresponding absolute value of motor impedance per-phase (refer 'Table-1') for the induction motor under test is computed as '24.1575(Ω)'. The magnitude of stator current per-phase, corresponding to combination 'no. 1' under 'Table-2,' is considered as reference value to represent the zero-percent (0%) state of degradation of insulation (viz., a 'healthy state'). In the following discussion, it is assumed that if the change in the value of stator current per-phase is within '25%' of the reference value then the value of stator current per-phase is considered in the low range (L). Similarly, if the change in the value is from '25%' to '60%' of the reference value then the value of stator current per-phase is considered in the medium range (M). Further, if the change in the value is above '60%' of the reference value then the value of stator current per-phase is considered in the high range (H).

The variations in the phase-shift displacements of electrical variables are measured with respect to reference with anticlockwise sense as positive. Any variation in phase-shift around and below '10°' in either direction is considered as negligible change in the phase-shift. Similarly, any variation in phase-shift within '10°' to '30°' in either direction is considered as moderate change in the phase-shift. Further, any variation in phase-shift over and above '30°' in either direction is considered as significant change in the phase-shift. The variation in the phase-shift displacements of quadrature-axis current variable is measured with respect to positive q-axis ('+90°'), with anticlockwise sense as positive over a dq-plane as shown in the Fig. 3.

4.1 Variable State of Degradation of Insulation in 'Phase-a' with Equal Intermediate State of Degradation of Insulation Present in 'Phase-b' and 'Phase-c'

The finite variation in the state of degradation of insulation, occurring in 'phase-a' and equal intermediate state of degradation of insulation present in 'phase-b' and 'phase-c,' will introduce the change in the shape of extended park's current data pattern from circular to elliptical form. The simulation results in 'Table-2,' inferred that the magnitudes of all the three phase currents (I_a , I_b , and I_c) are different and not displaced in time with each other by 120°. Similarly, the simulation results in 'Table-3,' inferred that the magnitudes of direct-axis and quadrature-axis current are not equal and not displaced in time with each other by '90°.' The resultant dq-axis current phasor (I_{dq}) is not displaced in time by '+45.0°' with respect to reference. The variations of electrical variables in either form are unlike to the case of equal variation in the state of degradation of insulation in all three phases.

4.1.1 Variable State of Degradation of Insulation in 'Phase-a' from Healthy to Intermediate State

It is imperative that, any variation in the state of degradation of insulation in 'phase-a' from healthy to intermediate state is always less than intermediate state of degradation present in the 'phase-b' and 'phase-c'. The graphical representations of extended park's current data pattern over a dq-plane for the selected number of combinations from '211' to '4211' (viz., '211, 2211, and 3411,' which are simulating '28.00%, 29.92%, and 32.40%' state of degradation of insulation, respectively) under 'Table-2, Table-3, and Table-4' are presented in Fig. 5.

The performance analysis of electrical variables in the three-phase machine model (abc) form (Refer 'Table-2'), equivalent two-phase model (dq) form (Refer 'Table-3'), and extracted mathematical parameters (Refer 'Table-4') for the variation in the state of degradation of insulation in 'phase-a' from healthy to intermediate state with equal intermediate state of degradation of insulation present in 'phase-b' and 'phase-c' is presented in the 'Table-5.'

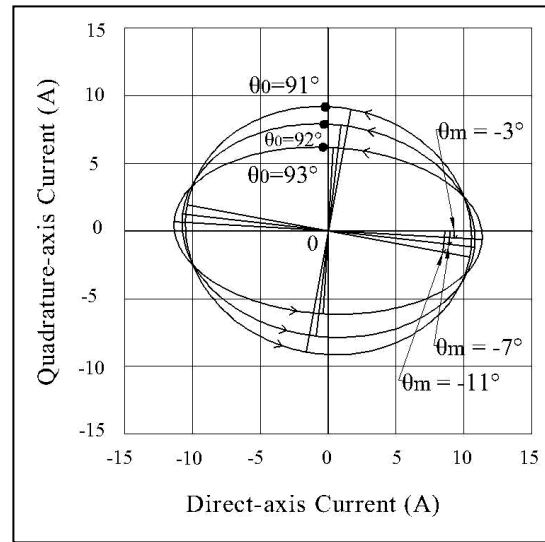


Fig. 5. Simulation of Variation in State of Degradation of Insulation in 'Phase-a' from Healthy to Intermediate State

4.1.2 Variable State of Degradation of Insulation in 'Phase-a' from Intermediate to Worst-Case State

It is imperative that, any variations in the state of degradation of insulation in 'phase-a' from intermediate to worst-case state is always more than intermediate state of degradation present in 'phase-b' and 'phase-c'. The graphical representations of extended park's current data pattern over a dq-plane for the selected number of combinations from '4211' to '7811' (viz., '5011, 6211, and 7811,' which are simulating '36.19%, 38.67%, and 40.46%' state of degradation of insulation, respectively) under 'Table-2, Table-3, and Table-4' are presented in Fig. 6.

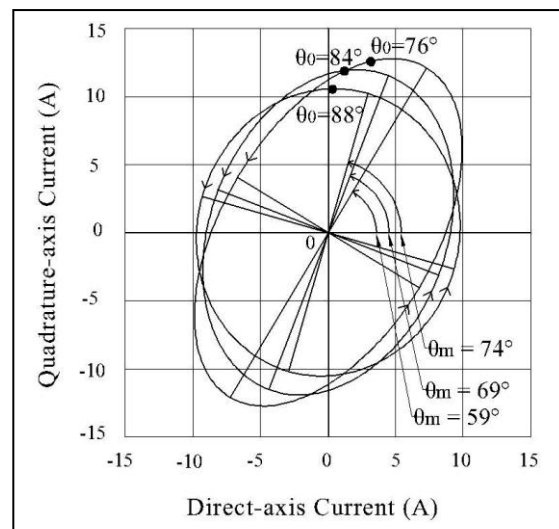


Fig. 6. Simulation of Variation in State of Degradation of Insulation in 'Phase-a' from Intermediate to Worst-Case State

TABLE 5

PERFORMANCE ANALYSIS FOR VARIABLE STATE OF DEGRADATION OF INSULATION IN PHASE-A FROM HEALTHY TO INTERMEDIATE STATE

Extracted Variable/Parameter	Performance Analysis
I_a, I_b, I_c	The magnitude of current in an affected 'phase-a' experiences a moderate increase and varies from low to medium range. The magnitude of current in lagging 'phase-b' experiences a negligible change (decrease) and varies within a medium range. The magnitude of current in leading 'phase-c' experiences a negligible increase and varies within a medium range.
$\beta_a, \beta_b, \beta_c$	In addition to affected 'phase-a' both lagging 'phase-b' as well as leading 'phase-c' current phasors experiences a moderate phase-shift in clockwise direction.
I_d, I_q, I_{dq}	' I_d ' experiences a negligible decrease and varies within a medium range. ' I_q ' experiences a moderate increase and varies from low to medium range. ' I_{dq} ' experiences negligible increase and varies within a medium range.
$\beta_d, \beta_q, \beta_{dq}$	The ' I_d ' phasor experiences a negligible phase-shift in anti-clockwise direction while the ' I_q ' phasor experiences a negligible phase-shift in clockwise direction. The ' I_{dq} ' phasor does have a moderate phase-shift in anti-clockwise direction.
$\theta_o^\circ, \theta_m^\circ$	The ' θ_o° ' changes its position over a negligible range (- 3.0°) in clockwise direction with respect to positive q-axis. It is shifted from ' $\theta_o^\circ = 93.0127^\circ$ ' (+93.0°) to ' $\theta_o^\circ = 90.0^\circ$ ' in clockwise direction with respect to reference. The ' θ_m° ' changes its position over a negligible range (- 8.0°) in clockwise direction with respect to reference. It is shifted from ' $\theta_m^\circ = - 3.6012^\circ$ ' (-3.0°) to ' $\theta_m^\circ = -10.7394^\circ$ ' (-11.0°) in clockwise direction with respect to reference.
L_{MA}, L_{MB}	The ' L_{MA} ' experience a negligible decrease (22.4046 to 19.8365) while ' L_{MB} ' moderately increases (12.3613 to 19.8365).
LR	The 'LR' significantly increases (6.8201 to 19.8365) with progressive rise in state of degradation of insulation in 'phase-a'.
ϵ	The deformation in an elliptic pattern changes with the variation in eccentricity from 0.8340 (close to '1') to 0.4782 (close to '0.5') with progressive rise in state of degradation of insulation in 'phase-a'.

The performance analysis of electrical variables in the three-phase machine model (abc) form (Refer 'Table-2'), equivalent two-phase model (dq) form (Refer 'Table-3'), and extracted mathematical parameters (Refer 'Table-4') for the variation in the state of degradation of insulation in 'phase-a' from intermediate to worst-case state with equal intermediate state of degradation of insulation present in 'phase-b' and 'phase-c' is presented in the 'Table-6.'

TABLE 6

PERFORMANCE ANALYSIS FOR VARIABLE STATE OF DEGRADATION OF INSULATION IN PHASE-A FROM INTERMEDIATE TO WORST-CASE STATE

Extracted Variable/Parameter	Performance Analysis
I_a, I_b, I_c	The magnitude of current in an affected 'phase-a' moderately increases from medium to high range. The magnitude of current in lagging 'phase-b' negligibly decreases and value varies within a medium range. The magnitude of current in leading 'phase-c' moderately increases and value varies from medium to high range.
$\beta_a, \beta_b, \beta_c$	The affected 'phase-a' experiences significant phase-shift in clockwise direction while lagging 'phase-b' as well as leading 'phase-c' experiences a moderate phase-shift in clockwise direction.
I_d, I_q, I_{dq}	' I_d ' experiences a negligible change (decrease/increase) and value varies within a medium range. ' I_q ' experiences a moderate increase and varies from medium to high range. ' I_{dq} ' experiences a significant increase and varies from medium to high range.
$\beta_d, \beta_q, \beta_{dq}$	The ' I_d ' phasor experiences a moderate phase-shift in anti-clockwise direction while the ' I_q ' phasor experiences a moderate phase-shift in clockwise direction. The ' I_{dq} ' phasor does have a negligible phase-shift in anti-clockwise direction.
$\theta_o^\circ, \theta_m^\circ$	The ' θ_o° ' changes its position over a moderate range (-14.0°) in clockwise direction with respect to positive q-axis. It is shifted from ' $\theta_o^\circ=90.0^\circ$ ' to ' $\theta_o^\circ=76.8389^\circ$ ' (+76.0°) in clockwise direction with respect to reference. The ' θ_m° ' changes its position over a moderate range (-15.0°) in clockwise direction with respect to reference. It is shifted from ' $\theta_m^\circ = + 73.8695^\circ$ ' (+74.0°) to ' $\theta_m^\circ = +59.8034^\circ$ ' (+59.0°) in clockwise direction with respect to reference.
L_{MA}, L_{MB}	The ' L_{MA} ' significantly increases (19.8365 to 29.2414) while ' L_{MB} ' moderately decreases (19.8365 to 15.2494).
LR	The 'LR' significantly decreases (19.8365 to 7.9525) with progressive rise in state of degradation of insulation in 'phase-a'.
ϵ	The deformation in an elliptic pattern changes with the variation in eccentricity from 0.4867 (close to '0.5') to 0.8533 (close to '1') with progressive rise in state of degradation of insulation in 'phase-a'.

4.2 Variable State of Degradation of Insulation in 'Phase-b' with Equal Intermediate State of Degradation of Insulation Present in 'Phase-c' and 'Phase-a'

The finite variation in the state of degradation of insulation, occurring in 'phase-b' and equal intermediate state of degradation of insulation present in 'phase-c' and 'phase-a', will introduce the change in the shape of extended park's current data pattern from circular to elliptical form. As mentioned in an earlier 'case-4.1,' the simulation results of electrical variables and extracted mathematical parameters for the present case are computed. On account of inadequate space, the simulated results are not shown in the present paper. However, the comparative performance analysis of the same is discussed and presented in the 'section-V.' It is imperative that, any variation in the state of degradation of

insulation in 'phase-b' from healthy to intermediate state is always less than intermediate state of degradation present in the 'phase-c' and 'phase-a.' The graphical representations of extended park's current data pattern over a dq-plane for the selected number of combinations (viz., '4011, 4111, and 4171,' which are simulating '28.00%, 29.92%, and 32.40%' state of degradation of insulation, respectively) are presented in Fig. 7.

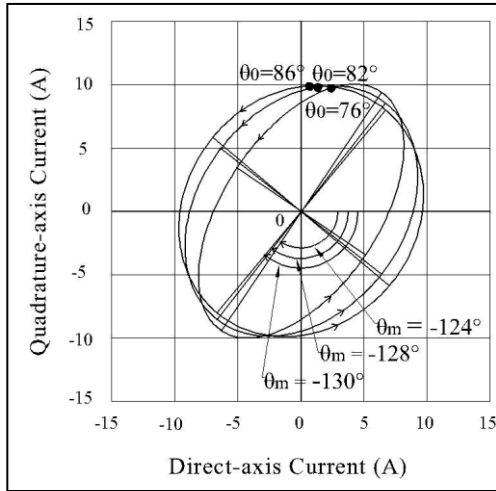


Fig. 7. Simulation of Variation in State of Degradation in 'Phase-b' from Healthy to Intermediate State

Contrary to this, any variation in the state of degradation of insulation in 'phase-b' from intermediate to worst-case state is always more than intermediate state of degradation present in 'phase-c' and 'phase-a.' The graphical representations of park's current pattern over a dq-plane for the selected number of combinations (viz., '4251, 4311, and 4391,' which are simulating '36.19%, 38.67%, and 40.46%' state of degradation of insulation, respectively) are presented in Fig. 8.

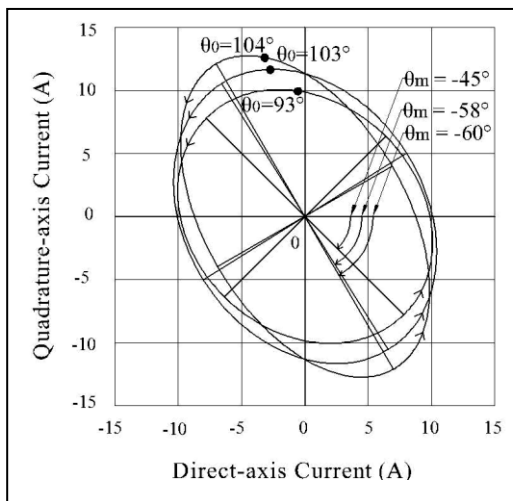


Fig. 8. Simulation of Variation in State of Degradation in 'Phase-b' from Intermediate to Worst-Case State

4.3 Variable State of Degradation of Insulation in 'Phase-c' with Equal Intermediate State of Degradation of Insulation Present in 'Phase-a' and 'Phase-b'

The finite variation in the state of degradation of insulation, occurring in 'phase-c' and equal intermediate state of degradation of insulation present in 'phase-a' and 'phase-b,' will change the shape of extended park's current data pattern from circular to elliptical form. As mentioned in an earlier 'case-4.1,' the simulation results of electrical variables and extracted mathematical parameters for the present case are computed. On account of inadequate space, the simulated results are not shown in the present paper. However, the comparative performance analysis of the same is discussed and presented in the 'section-5.' It is imperative that, any variation in the state of degradation of insulation in 'phase-c' from healthy to intermediate state is always less than intermediate state of degradation present in the 'phase-a' and 'phase-b.' The graphical representations of extended park's current data pattern over a dq-plane for the selected no. of combinations (viz., '4201, 4206, and 4209,' which are simulating '28.00%, 29.92%, and 32.40%' state of degradation of insulation, respectively) are presented in Fig. 9.

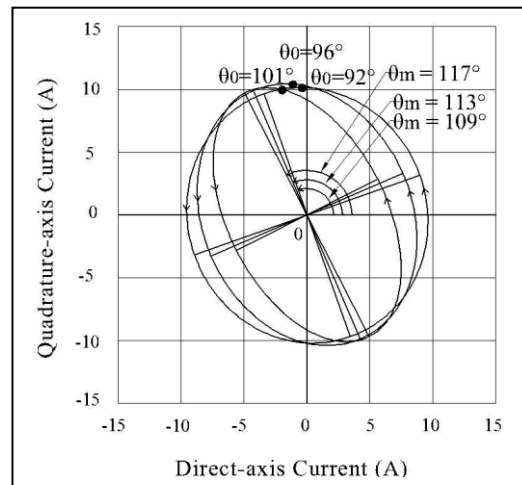


Fig. 9. Simulation of Variation in State of Degradation in 'Phase-c' from Healthy to Intermediate State

Contrary to this, any variation in the state of degradation of insulation in 'phase-c' from intermediate to worst-case state is always more than intermediate state of degradation present in 'phase-a' and 'phase-b.' The graphical representations of extended park's current data pattern over a dq-plane for the selected no. of combinations (viz., '4213, 4216, and 4220,' which are simulating '36.19%, 38.67%, and 40.46%' state of degradation of insulation, respectively) are presented in Fig. 10.

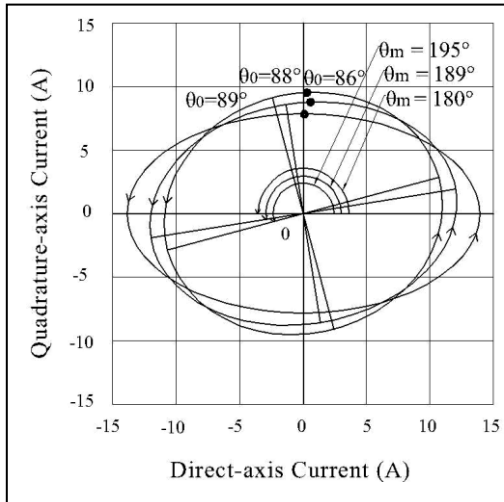


Fig. 10. Simulation of Variation in State of Degradation in 'Phase-c' from Intermediate to Worst-Case State

5 DISCUSSION ON PERFORMANCE ANALYSIS

The progressive rise in an equal state of degradation of insulation in all the three-phases results into the significant increase in the magnitudes of three-phase currents. Further, all the three-phase current phasors experiences a significant phase-shift in the clockwise direction but are still displaced in time with each other by 120°. In an equivalent two-phase (dq) model, the magnitudes of both 'direct-axis', and 'quadrature-axis' current significantly increases, and are equal. However, there is no change in the phase-shift ($\beta_d = 0^\circ$ and $\beta_q = +90^\circ$) for either one of them. The quadrature-axis current phasor is

always leading in quadrature with direct-axis current phasor over a dq-plane. Hence, the extended park's current data pattern appears in the circular form with significant rise in its radius.

If intermediate state of degradation of insulation is present in any two-phases, and the state of degradation of insulation, occurring in the remaining phase progressively increases from healthy to intermediate state (viz., 'part-(4.1.1) of 'case-4.1,' under 'section-4') then the extended parks current data pattern appears in elliptic form. The magnitudes of all the three phase currents (I_a , I_b , and I_c) are different and they are not displaced in time with each other by 120°. The magnitude of current in an 'affected-phase' experiences a moderate increase in its value and varies from low to medium range. The magnitude of current in the 'lagging-phase' experiences a negligible change (decrease) in its value and varies within a medium range. The magnitude of current in the 'leading-phase' experiences a negligible increase in its value and varies within a medium range. In addition to 'affected-phase' both 'lagging-phase' as well as 'leading-phase' current phasors experiences a moderate phase-shift in clockwise direction.

The comparative performance analysis of simulated electrical variables in equivalent two-phase dq-model form is detailed in 'Table-7.' The changes in magnitudes and phase-shift angles of direct-axis, quadrature-axis, and resultant dq-axis currents are varying over a different range to distinguish the presence of intermediate state of degradation of insulation in any two-phases and variation in the state of degradation of insulation (from healthy to intermediate state), in the remaining phase.

TABLE 7

COMPARATIVE PERFORMANCE ANALYSES OF SIMULATED ELECTRICAL VARIABLES IN EQUIVALENT TWO-PHASE (DQ) MODEL FORM FOR INTERMEDIATE STATE OF DEGRADATION OF INSULATION PRESENT IN ANY TWO-PHASES AND VARIATION FROM HEALTHY TO INTERMEDIATE STATE OF DEGRADATION IN REMAINING PHASE.

Variation in Degraded Phase	Other Two-Phases	Magnitude of Currents (A)			Phase Shift of Currents (°)		
		I_d (A)	I_q (A)	I_{dq} (A)	β_d (°)	β_q (°)	β_{dq} (°)
a	b-c (b-c > a)	(M) Negligible Decrease (11.18→9.91) (↓)	(L to M) Moderate Increase (6.2→9.91) (↑)	(M) Negligible Increase (12.35→14.02) (↑)	Negligible (anti-clockwise) (-2° → 0°)	Negligible (clockwise) (+93° → +90°)	Moderate (anti-clockwise) (+28° → +45°)
b	c-a (c-a > b)	(M) Negligible Increase (8.05→9.91) (↑)	(M) Negligible Change (↓↑) (9.93→9.72→9.91)	(H to M) Negligible Decrease (15.62→14.02) (↓)	Moderate (clockwise) (+17° → 0°)	Moderate (anti-clockwise) (+76° → +90°)	Negligible (clockwise) (+50° → +45°)
c	a-b (a-b > c)	(L to M) Moderate Increase (7.44→9.91) (↑)	(M) Negligible Change (↓) (10.4→9.91) (↓)	(L to M) Moderate Increase (9.7→14.02) (↑)	Moderate (anti-clockwise) (-16° → +0°)	Moderate (clockwise) (+101° → +90°)	Moderate (clockwise) (+58° → +45°)

Similarly, the comparative performance analyses of corresponding simulated extracted parameters are detailed in 'Table-8' and 'Table-9.' With reference to 'Table-8,' it is observed that the extracted parameter like angle of orientation (θ_0) of an elliptic pattern (locus), changes its position over a

variable range. It is changing over different zones (viz., '+93.0° to +90.0°, +76.0° to +90.0°, and +102.0° to +90.0°') in a dq-plane, for intermediate state of degradation of insulation present in any two-phases (viz., b-c, c-a, and a-b) and variation in the state of degradation of insulation (from healthy to intermediate state), in the remaining affected-phase (viz., a, b, and c), respectively. This is illustrated in Fig. 11.

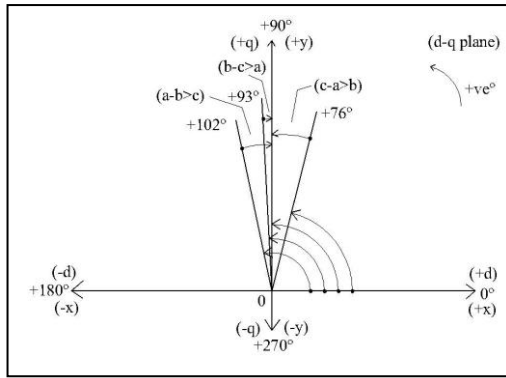


Fig. 11. Different Zones of Angle of Orientation (θ_0°) for Healthy to Intermediate State of Degradation of Insulation in Affected Phase

With reference to 'Table-8,' it is observed that the extracted parameter like angle of major-axis (θ_m°) of an elliptic pattern, changes its position over a negligible range (-8.0°), which is identical irrespective of intermediate state of degradation of insulation present in any two-phases (viz., b-c, c-a, and a-b) and variation in the state of degradation of insulation (from healthy to intermediate state) in the remaining affected-phase (viz., a, b, and c) respectively. However, ' θ_m° ' is changing over distinct zones (viz., ' -3.0° to -11.0° , -123.0° to -130.0° , and $+117.0^\circ$ to $+109.0^\circ$ ') in a dq-plane, for intermediate state of degradation of insulation present in any two-phases (viz., b-c, c-a, and a-b) and variation in the state of degradation of insulation (from healthy to intermediate state) in the remaining affected-phase (viz., a, b, and c), respectively. This is illustrated in Fig. 12.

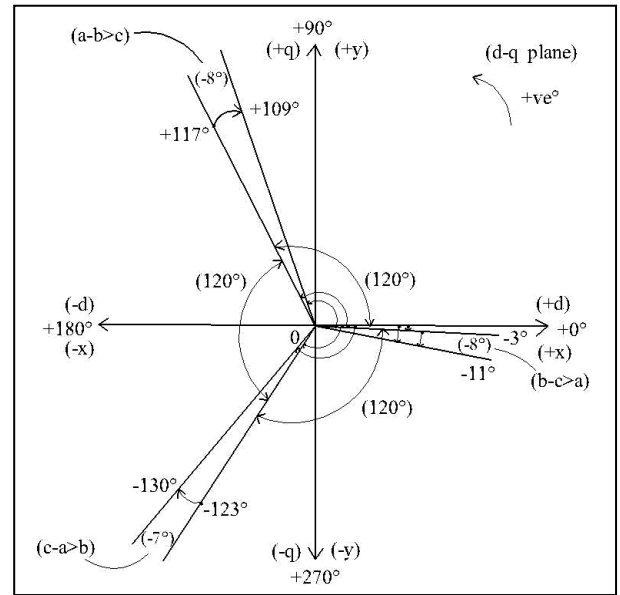


Fig. 12. Distinct Zones of Angle of Major-Axis (θ_m°) for Healthy to Intermediate State of Degradation of Insulation in Affected Phase

With reference to 'Table-9,' it is observed that the changes in an extracted parameters like ' L_{MA} , L_{MB} , LR, and ϵ ' are identical, which occur irrespective of an intermediate state of degradation of insulation present in any two-phases (viz., b-c, c-a, and a-b) and variation in the state of degradation of insulation (from healthy to intermediate state), in the remaining affected-phase (viz., a, b, and c), respectively.

TABLE 8

COMPARATIVE PERFORMANCE ANALYSES OF SIMULATED EXTRACTED PARAMETERS ' θ_0° ' AND ' θ_m° ,' FOR INTERMEDIATE STATE OF DEGRADATION OF INSULATION PRESENT IN ANY TWO-PHASES AND VARIATION FROM HEALTHY TO INTERMEDIATE STATE OF DEGRADATION IN REMAINING PHASE.

Variation in Degraded Phase	Other Two-Phases	Angle of Orientation (θ_0°)	Range of Angle of Orientation (θ_0°)	Angle of Major-Axis (θ_m°)	Range of Angle of Major-Axis (θ_m°)
a	b-c (b-c > a)	(+93.0°) to (+90.0°)	Negligible (-3.0°) clockwise	(-3.0°) to (-11.0°)	Negligible (-8.0°) clockwise
b	c-a (c-a > b)	(+76.0°) to (+90.0°)	Moderate (+14.0°) anti-clockwise	(-123.0°) to (-130.0°)	Negligible (-7.0°) clockwise
c	a-b (a-b > c)	(+102.0°) to (+90.0°)	Moderate (-12.0°) clockwise	(+117.0°) to (+109.0°)	Negligible (-8.0°) clockwise

TABLE 9

COMPARATIVE PERFORMANCE ANALYSES OF SIMULATED EXTRACTED PARAMETERS 'L_{MA}, L_{MB}, E, AND LR,' FOR INTERMEDIATE STATE OF DEGRADATION OF INSULATION PRESENT IN ANY TWO-PHASES AND VARIATION FROM HEALTHY TO INTERMEDIATE STATE OF DEGRADATION IN REMAINING PHASE.

Variation in Degraded Phase	Other Two-Phases	Length of Major-Axis (L _{MA})	Length of Minor-Axis (L _{MB})	Eccentricity (ε)	Latus Rectum (LR)
a	b-c (b-c > a)	Negligible Decrease (22.4046→19.8365) (↓)	Moderate Increase (12.3613→19.8365) (↑)	0.8340 (close to '1') to 0.4782 (cl. to 0.5')	Significant Increase (6.8201→19.8365) (↑)
b	c-a (c-a > b)	Negligible Decrease (22.4038→19.8365) (↓)	Moderate Increase (12.3628→19.8365) (↑)	0.8340 (close to '1') to 0.4781 (cl. to '0.5')	Significant Increase (6.8220→19.8365) (↑)
c	a-b (a-b > c)	Negligible Decrease (22.4038→19.8365) (↓)	Moderate Increase (12.3628→19.8365) (↑)	0.8340 (close to '1') to 0.4782 (cl. to '0.5')	Significant Increase (6.8220→19.8365) (↑)

If intermediate state of degradation of insulation is present in any two-phases, and the state of degradation of insulation, occurring in the remaining phase progressively increases from intermediate to worst-case state (viz., 'part-(4.1.2)' of 'case-4.1,' under 'section-4') then the extended parks current data pattern appears in an elliptic form. The magnitude of all the three phase currents (I_a, I_b, and I_c) are different and they are not displaced in time with each other by 120°. The magnitude of current in an 'affected-phase' and 'leading-phase' experiences a moderate increase in their values and varies from medium to high range. The magnitude of current in the 'lagging-phase' experiences a negligible decrease in its value and varies within a medium range. The 'affected-phase' current phasor experiences a significant phase-shift in clockwise direction

whereas 'lagging-phase' as well as 'leading-phase' current phasors experiences a moderate phase-shift in clockwise direction.

The comparative performance analysis of simulated electrical variables in equivalent two-phase (dq) model form is detailed in 'Table-10.' The changes in magnitudes and phase-shift angles of direct-axis, quadrature-axis, and resultant dq-axis currents are varying over a different range to distinguish the presence of intermediate state of degradation of insulation in any two-phases and variation in the state of degradation of insulation (from intermediate to worst-case state) in the remaining phase.

TABLE 10

COMPARATIVE PERFORMANCE ANALYSES OF SIMULATED ELECTRICAL VARIABLES IN EQUIVALENT TWO-PHASE (DQ) MODEL FORM FOR INTERMEDIATE STATE OF DEGRADATION OF INSULATION PRESENT IN ANY TWO-PHASES AND VARIATION FROM INTERMEDIATE TO WORST-CASE STATE OF DEGRADATION IN REMAINING PHASE.

Variation in Degraded Phase	Other Two-Phase s	Magnitude of Currents (A)			Phase Shift of Currents (°)		
		I _d (A)	I _q (A)	I _{dq} (A)	β _d (°)	β _q (°)	β _{dq} (°)
a (a>b-c)	b-c	(M) Negligible Change (↓↑) (9.9→9.36→9.82)	(M to H) Moderate Increase (9.91→13.24) (↑)	(M to H) Significant Increase (14.02→20.15) (↑)	Moderate (anti-clockwise) (0° → +18°)	Moderate (clockwise) (+90° → +76°)	Negligible (anti-clockwise) (+45° → 53°)
b (b>c-a)	c-a	(M) Negligible Change (↑↓) (9.9→10.4→9.87)	(M to H) Moderate Increase (9.91→13.20) (↑)	(M) Moderate Decrease (14.02→11.67) (↓)	Moderate (clockwise) (0° → -18°)	Moderate (anti-clockwise) (+90° → +104°)	Moderate (anti-clockwise) (+45° → 57°)
c (c>a-b)	a-b	(M to H) Moderate Increase (9.91→14.62) (↑)	(M to L) Moderate Decrease (9.91→7.62) (↓)	(H) Negligible Increase (14.02→16.52) (↑)	Negligible (clockwise) (+0° → 3° → +0°)	Negligible (anti-clockwise) (+90° → +86° → +90°)	Moderate (clockwise) (+45° → 27°)

Similarly, the comparative performance analyses of corresponding simulated extracted parameters are detailed in 'Table-11' and 'Table-12.' With reference to 'Table-9,' it is observed that the angle of orientation (θ₀) of an elliptic pattern (locus), changes its position over a variable range. It is changing over different zones (viz., '+90.0 ° to +76.0 °, +90.0° to +104.0°, and +90.0° to +86.0 °') in a dq-plane, for

intermediate state of degradation of insulation present in any two-phases (viz., b-c, c-a, and a-b) and variation in the state of degradation of insulation (from intermediate to worst-case state) in the remaining affected-phase (viz., a, b, and c), respectively. This is illustrated in Fig. 13.

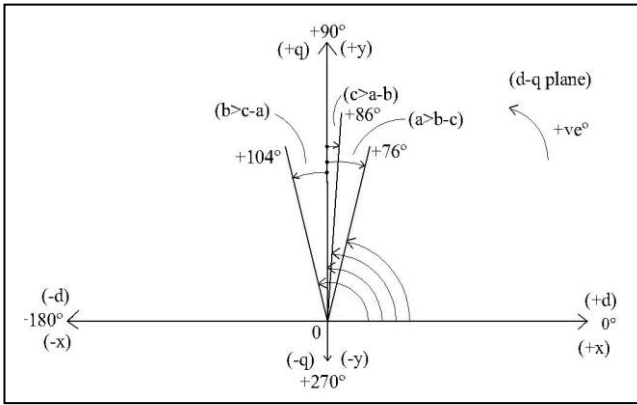


Fig. 13. Different Zones of Angle of Orientation (θ_0°) for Intermediate to Worst-Case State of Degradation of Insulation in Affected Phase

With reference to 'Table-9,' it is observed that the angle of major-axis (θ_m°) of an elliptic pattern, changes its position over a moderate range (-15.0°), which is identical irrespective of the intermediate state of degradation of variation in the state of degradation of insulation (from intermediate to worst-case state) in any remaining affected-phase (viz., a, b, and c) respectively. However, ' θ_m° ' is changing over distinct zones (viz., '+74.0 ° to +59.0 °, - 45.0 ° to - 60.0°, and +195.0° to +180.0°') in a dq-plane, for intermediate state of degradation of insulation present in any two-phases (viz., b-c, c-a, and a-b) and variation in the state of degradation of insulation (from intermediate to worst-case state) in the remaining affected-phase (viz., a, b, and c), respectively. This is illustrated in Fig. 14.

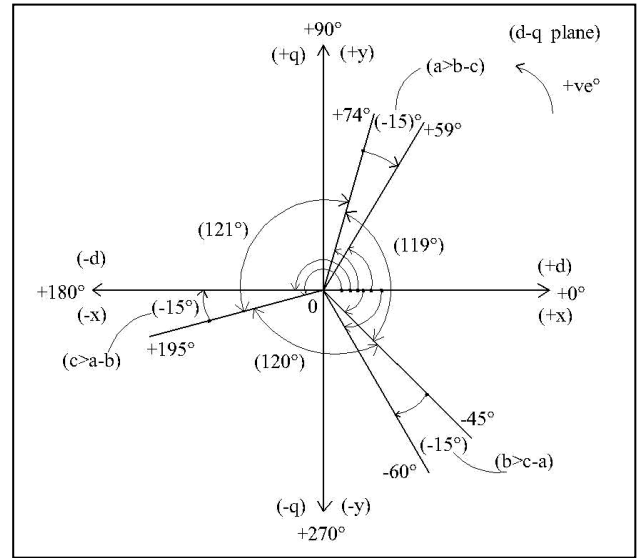


Fig. 14. Distinct Zones of Angle of Major-Axis (θ_m°) for Intermediate to Worst-Case State of Degradation of Insulation in Affected Phase

With reference to 'Table-12,' it is observed that the changes in an extracted parameters like ' L_{MA} , L_{MB} , LR , and ϵ ' are identical, which occur irrespective of intermediate state of degradation of insulation present in any two-phases (viz., b-c, c-a, and a-b) and variation in the state of degradation of insulation (from intermediate to worst-case state) in the remaining affected-phase (viz., a, b, and c) respectively.

TABLE 11

COMPARATIVE PERFORMANCE ANALYSES OF SIMULATED EXTRACTED PARAMETERS ' θ_0° ' AND ' θ_m° ,' FOR INTERMEDIATE STATE OF DEGRADATION OF INSULATION PRESENT IN ANY TWO-PHASES AND VARIATION FROM INTERMEDIATE TO WORST-CASE STATE OF DEGRADATION IN REMAINING PHASE.

Variation in Degraded Phase	Other Two-Phases	Angle of Orientation (θ_0°)	Range of Angle of Orientation (θ_0°)	Angle of Major-Axis (θ_m°)	Range of Angle of Major-Axis (θ_m°)
a (a>b-c)	b-c	(+90.0°) to (+76.0°)	Moderate (- 14.0°) clockwise	(+74.0°) to (+59.0°)	Moderate (-15.0°) clockwise
b (b>c-a)	c-a	(+90.0°) to (+104.0°)	Moderate (+14.0°) anti-clockwise	(- 45.0°) to (- 60.0°)	Moderate (-15.0°) clockwise
c (c>a-b)	a-b	(+90.0°) to (+86.0°)	Negligible (-4.0°) clockwise	(+195.0°) to (+180.0°)	Moderate (-15.0°) clockwise

TABLE 12

COMPARATIVE PERFORMANCE ANALYSES OF SIMULATED EXTRACTED PARAMETERS 'L_{MA}, L_{MB}, E, AND LR,' FOR INTERMEDIATE STATE OF DEGRADATION OF INSULATION PRESENT IN ANY TWO-PHASES AND VARIATION FROM INTERMEDIATE TO WORST-CASE STATE OF DEGRADATION IN REMAINING PHASE.

Variation in Degraded Phase	Other Two-Phases	Length of Major-Axis (L _{MA})	Length of Minor-Axis (L _{MB})	Eccentricity (ε)	Latus Rectum (LR)
a (a>b-c)	b-c	Significant Increase (19.8365→29.2414) (↑)	Moderate Decrease (19.8365→15.2494) (↓)	0.4867 (cl. to '0.5') to 0.8533 (close to '1')	Significant Decrease (19.8365→7.9525) (↓)
b (b>c-a)	c-a	Significant Increase (19.8365→29.2433) (↑)	Moderate Decrease (19.8365→15.2457) (↓)	0.4866 (cl. to '0.5') to 0.8533 (close to '1')	Significant Decrease (19.8365→7.9482) (↓)
c (c>a-b)	a-b	Significant Increase (19.8365→29.2435) (↑)	Moderate Decrease (19.8365→15.2453) (↓)	0.4867 (cl. to '0.5') to 0.8534 (close to '1')	Significant Decrease (19.8365→7.9477) (↓)

6 CONCLUSIONS

In the present work, the computer simulation model is developed to simulate arbitrary variations in the state of degradation of stator groundwall insulation, occurring in the respective phases of induction motor under test. An extended park's transformation model is used to transform the simulation results from three-phase ('abc') model into a more convenient and simplified form of equivalent two-phase ('dq') model over a dq-plane. Extended park's current data patterns are derived from two-phase ('dq') model to distinguish the state of degradation of insulation. The performance analysis of electrical variables and extracted parameters of extended park's current data patterns for particular case is concluded here.

6.1 Equal Intermediate State of Degradation Present in Any Two-Phases with Variable State of Degradation from Healthy to Intermediate state in Remaining Phase

An equal intermediate state of degradation of insulation present in any two-phases is always more dominant as compared to the progressive increase in the state of degradation from healthy to intermediate state in the remaining phase. As detailed in 'Table-7,' the magnitude (I_d, I_q, and I_{dq}) and phase-shift angle (β_d, β_q, and β_{dq}) of electrical variables in the equivalent two-phase (dq) model form responds in distinct manner for equal intermediate state of degradation of insulation present in any two-phases (viz., b-c, c-a, and a-b) with progressive increase in the state of degradation from healthy to intermediate state in the remaining phase (viz., a, b, and c), respectively.

In the forgoing discussion, the Fig. 11 illustrates the change in the angle of orientation (θ₀^o) of an elliptic pattern (locus) over a dq-plane. It is imperative that the variation in 'θ₀^o' is symmetrical and limited over a small range with respect to positive 'q-axis.' Similarly, the Fig. 12 illustrates the change in the angle of major-axis (θ_m^o) of an elliptic pattern over a dq-plane. It is imperative that the variation in 'θ_m^o' is

symmetrically distributed by '120^o' over distinct zones, in a dq-plane. It further suggests that these extracted parameters are sensitive within these specific limits in context of progressive increase in the state of degradation of insulation (from healthy to intermediate state) in any one particular phase (viz., a, b, and c) and dominant equal intermediate state of degradation present in other two-phases (viz., b-c, c-a, and a-b), respectively. As detailed in 'Table-9,' the changes in the corresponding extracted parameters like 'L_{MA}, L_{MB}, LR, and ε' are identical, irrespective of progressive increase in the state of degradation of insulation (from healthy to intermediate state), in any one particular phase (viz., a, b, and c) and dominant equal intermediate state of degradation present in other two-phases (viz., b-c, c-a, and a-b), respectively. The changes in extracted parameters like 'L_{MA}, L_{MB}, and LR' further suggests that the deformation in the shape of extended park's current elliptic pattern decreases with the change in an eccentricity (ε) from '0.8340' viz., close to one (1) to '0.4782' viz., close to mid-value (0.5).

6.2 Equal Intermediate State of Degradation Present in Any Two-Phases with Variable State of Degradation from Intermediate to Worst-case state in Remaining Phase

An equal intermediate state of degradation of insulation present in any two-phases is always less as compared to any progressive increase in the state of degradation from intermediate to worst-case state in the remaining phase. As detailed in 'Table-10,' the magnitude (I_d, I_q, and I_{dq}) and phase-shift angle (β_d, β_q, and β_{dq}) of electrical variables in the equivalent two-phase (dq) model form responds in distinct manner for equal intermediate state of degradation of insulation present in any two-phases (viz., b-c, c-a, and a-b) with progressive increase in the state of degradation from intermediate to worst-case state in the remaining phase (viz., a, b, and c), respectively.

In the forgoing discussion, the Fig. 13 illustrates the change in the angle of orientation (θ₀^o) of an elliptic pattern (locus) over a dq-plane. It is imperative that the variation in 'θ₀^o' is symmetrical and limited over a small range with respect to positive 'q-axis.' Similarly, the Fig. 14 illustrates the change in

the angle of major-axis (θ_m°) of an elliptic pattern over a dq-plane. It is imperative, that the variation in ' θ_m° ' is symmetrically distributed by ' 120° ' over distinct zones, in a dq-plane. It further suggests that these extracted parameters are sensitive within these specific limits in context of progressive increase in the state of degradation of insulation (from intermediate to worst-case state) in any one particular phase (viz., a, b, and c) and less dominant equal intermediate state of degradation present in other two-phases (viz., b-c, c-a, and a-b), respectively. As detailed in 'Table-12,' the changes in the corresponding extracted parameters like ' L_{MA} , ' L_{MB} , LR, and ϵ' ' are identical, irrespective of a dominant progressive increase in the state of degradation of insulation (from intermediate to worst-case state) in any one particular phase (viz., a, b, and c) and equal intermediate state of degradation of insulation present in other two-phases (viz., b-c, c-a, and a-b), respectively. The changes in extracted parameters like ' L_{MA} , ' L_{MB} , and LR' further suggests that the deformation in the shape of extended park's current elliptic pattern increases with the change in an eccentricity (ϵ) from '0.4867' viz., close to mid-value (0.5) to '0.8533' viz., close to one (1).

The extracted parameter like eccentricity (ϵ) is not sufficient to decide the level of state of degradation of insulation. In fact, it only suggests the deformation in the shape of extended park's current elliptic pattern and in turn suggests the degree of unbalance in the three phase stator current. The extracted parameter like length of major-axis (L_{MA}), length of minor-axis (L_{MB}), and latus rectum (LR) suggests the size of extended park's current elliptic pattern and in turn are sensitive to decide level of state of degradation of insulation. Hence, extracted parameters like ' L_{MA} , ' L_{MB} , LR, and ϵ' ' are useful to uniquely determine the qualitative level of variations (low, medium, and high etc.) of an intermediate state of degradation of stator groundwall insulation present in any two-phases, and progressive increase in the state of degradation of insulation, occurring in the remaining phase.

REFERENCES

- [1] G. C. Stone, H. G. Sedding, B.A. Lloyd, and B.K. Gupta, "The ability of diagnostic tests to estimate the remaining life of stator insulation," *IEEE Trans. Energy Conversion*, vol.3, no.4, pp. 833 – 841, Dec.1988.
- [2] T. Tsukui, M. Takamura, and Y. Kako, "Correlations between Nondestructive and Destructive Tests on High-Voltage Coil Insulations for Rotating Machines," *IEEE Trans. Electrical Insulation*, vol. 15, no. 2, pp. 118-124, April 1980.
- [3] A. J. Modak and H.P. Inamdar, "Computer-Aided Characteristic Simulation Model of Deterioration of Insulation of Induction Motor," *Proc. 3rd IEEE Int. Conf. Computer and Electrical Engineering*, IEEE Press, UESTC, Chengdu, China, Nov. 16-18 2010, vol.11, pp. VII-569-574. (ISBN: 978-1-4244-7224-6).

- [4] N. Arthur and J. Penman, "Induction machine conditioning monitoring with higher order spectra," *IEEE Trans. Ind. Elect.*, vol.47, no.5, pp. 1031-1041, Oct. 2000.
- [5] F. Filippetti, G. Franceschini, C. Tassoni, and Peter Vas, "Recent developments of induction motor drives fault diagnosis using AI techniques," *IEEE Trans. Ind. Elect.*, vol.47, no.5, pp. 994-1004, Oct. 2000.
- [6] F. C. Trutt *et al.*, "Detection of AC machine winding deterioration using electrically excited vibrations," *IEEE Trans. Ind. Applications*, vol.17, no.1, pp. 10 -13, Jan. / Feb. 2001.
- [7] A. J. M. Cardoso *et al.*, "Computer aided detection of air gap eccentricity in operating three phase induction motors by Park's vector approach," *IEEE Trans. Ind. Applications*, vol.29, pp. 897-901, Sept. / Oct. 1993.
- [8] A. J. M. Cardoso *et al.*, "Inter turn stator winding fault diagnosis in three phase induction motors, by Park's vector approach," *IEEE Trans. Energy Conversion*, vol.14, no. 3, pp. 595-598, Sept.1999.